D. B. Bogy N. Bugdayci F. E. Talke

# **Experimental Determination of Creep Functions for Thin Orthotropic Polymer Films**

Stringent requirements on the dimensional stability of polymer films used as substrates for magnetic recording make it necessary to experimentally determine their anisotropic viscoelastic behavior. This paper deals with the measurement of the time-dependent, longitudinal elongation and lateral contraction of 50 × 900-mm biaxially oriented orthotropic polyethylene terephthalate (PET) strips. Two different methods are described for measuring longitudinal elongation, and a laser-scanning technique is used for measuring lateral contraction. Preliminary investigations are carried out to determine the static Poisson's ratio, to check the linearity of longitudinal creep with respect to load, and to investigate the validity of the time-temperature superposition hypothesis. In addition, tests are described in which longitudinal and lateral creep of the specimens are simultaneously measured under constant loads in temperature- and humidity-controlled environments. It is found that the Poisson's ratio has only a weak dependence on time, and, therefore, a good approximation may be obtained by treating the Poisson's ratio as independent of time.

#### Introduction

When thin films are used as substrates for magnetic recording, the requirements on dimensional stability become increasingly stringent as the density of stored information is increased. Geometric distortion of the data tracks either limits the track density or necessitates the use of complicated servo systems. Thus, the amount of deformation to be expected of a substrate in a particular design configuration is of special interest.

Dimensional changes occur in polymer films with changes in temperature, humidity, and internal structure. Deformation also results from the mechanical loading inherent in the physical configurations in which the media are used. Such deformation may appear to be elastic if the duration of loading is short, but otherwise most polymer films behave viscoelastically. In particular, they creep under applied load and partially recover when the loading is removed. Therefore, the determination of creep functions in controlled environments is needed for calculating the amount of distortion apt to occur in any machine configuration. A further distortion results due to the fact that

considerable stretching in one or more directions is employed by the manufacturer to give polymer sheets the desired strength properties. This stretching orients the molecules and results in a directional dependence of the physical properties of the medium. Thus, the sheets are anisotropic but usually have in-plane orthotropic symmetry, *i.e.*, there are two perpendicular axes of material symmetry. As a result of the stretching there occurs for a considerable period of time a partial viscoelastic recovery. At room temperature this recovery can continue for many months.

Design data published by the manufacturers of these oriented sheets usually assume the material to be isotropic and elastic [1], and for many applications this is satisfactory. However, when these sheets are used as substrates for magnetic recording, the anisotropy and viscoelasticity must be taken into account for the reasons stated, and the appropriate material properties need to be determined experimentally. The complete characterization of these orthotropic films requires the experimen-

Copyright 1979 by International Business Machines Corporation. Copying is permitted without payment of royalty provided that (1) each reproduction is done without alteration and (2) the *Journal* reference and IBM copyright notice are included on the first page. The title and abstract may be used without further permission in computer-based and other information-service systems. Permission to *republish* other excerpts should be obtained from the Editor.

tal determination of four viscoelastic creep functions (in place of two for isotropic), two coefficients of thermal expansion (in place of one), and two coefficients of hygroscopic expansion (in place of one). In addition to the knowledge of these material properties, from which we can calculate the deformations expected from environmental changes and configurational loading, we must also determine experimentally the amount of "free shrinkage recovery."

Some work has been done on the anisotropic elastic properties of polymers (i.e., for short duration observations) [2], but only recently have anisotropic viscoelastic creep functions begun to appear in the literature [3-5], and these are for much thicker samples than the films used for substrates. It is important to realize that the properties of oriented polymers may vary widely between blocks and thin films, since their processes of manufacture are generally quite different. For this reason, it is necessary to conduct tests on specimens taken directly from thin sheets as obtained from the industrial suppliers and to catalog the properties according to the particular manufacturing process. Some work of this nature has been carried out by various research groups in IBM. At IBM Research, San Jose, experimental thermomechanical analysis has been carried out by Barrall and Logan [6] to determine thermal expansion coefficients of PET sheets. Smith [7] has obtained some longitudinal creep function data, but the apparatus used cannot simultaneously measure lateral contraction. At IBM's General Products Division, Boulder, Bartkus [8] has conducted experiments to determine biaxial hygroscopic expansion coefficients, and Bartkus and Price [9] have studied the shrinkage problem. The material properties obtained in these studies have been used by Bogy [10] to make theoretical estimates of distortion in rotating PET disks. Finally, the creep of such a disk has been measured experimentally by H. J. Greenberg [11] at IBM Research, San Jose.

It can be shown [12, 13] that the linear viscoelastic strain-stress relation for deformation in the plane of a thin homogeneous orthotropic film may be written as

$$\begin{split} & \varepsilon_{11}(x, t) \\ & = \int_{-\infty}^{t} \left[ J_{11}(t - \tau) \frac{\partial \sigma_{11}}{\partial \tau}(x, \tau) + J_{12}(t - \tau) \frac{\partial \sigma_{22}}{\partial \tau}(x, \tau) \right] d\tau, \\ & \varepsilon_{22}(x, t) \\ & = \int_{-\infty}^{t} \left[ J_{12}(t - \tau) \frac{\partial \sigma_{11}}{\partial \tau}(x, \tau) + J_{22}(t - \tau) \frac{\partial \sigma_{22}}{\partial \tau}(x, \tau) \right] d\tau, \\ & \varepsilon_{12}(x, t) = \frac{1}{2} \int_{-\infty}^{t} J_{66}(t - \tau) \frac{\partial \sigma_{12}}{\partial \tau}(x, \tau) d\tau, \end{split}$$
(1)

where x stands for the coordinates  $x_1$ ,  $x_2$  of a point in the sheet; t (and  $\tau$ ) is time;  $\varepsilon_{11}$ ,  $\varepsilon_{22}$ ,  $\varepsilon_{12}$  are strain components;  $\sigma_{11}$ ,  $\sigma_{22}$ ,  $\sigma_{12}$  are stress components; and  $J_{11}$ ,  $J_{12}$ ,  $J_{22}$ ,  $J_{66}$  are the four viscoelastic creep compliances that characterize the material. The form of (1) is correct provided the coordinate axes are aligned with the material symmetry axes. For creep under uniform constant uniaxial stress  $\sigma$ , (1) becomes

$$\varepsilon_{11}(t) = J_{11}(t)\sigma, \qquad \varepsilon_{22}(t) = J_{12}(t)\sigma \tag{2}$$

for  $\sigma$  in the x<sub>1</sub>-direction and

$$\varepsilon_{11}(t) = J_{12}(t)\sigma, \qquad \varepsilon_{22}(t) = J_{22}(t)\sigma \tag{3}$$

for  $\sigma$  in the  $x_2$ -direction. Thus, by measuring the longitudinal extension and lateral contraction of tension specimens cut along each of the two symmetry axes of the material, we can determine  $J_{11}(t)$ ,  $J_{22}(t)$ , and  $J_{12}(t)$ . If the specimen is cut at an angle  $\phi$  with the  $x_1$ -axis, the tensor transformation law and the elastic-viscoelastic correspondence principle give, for the Laplace transform of the tensile compliance in the  $\phi$ -direction,

$$\bar{J}_{\phi}(s) = \bar{J}_{11}(s) \cos^4 \phi + [\bar{J}_{66}(s) - 2\bar{J}_{12}(s)] \sin^2 \phi \cos^2 \phi 
+ \bar{J}_{20}(s) \sin^4 \phi,$$
(4)

where  $\bar{J}(s)$  denotes the Laplace transform of J(t). Therefore, we can determine  $J_{66}(t)$  from the knowledge of  $J_{11}(t)$ ,  $J_{22}(t)$ ,  $J_{12}(t)$  and  $J_{\phi}(t)$ . It follows that at least three tensile creep tests are required and the lateral contraction must also be measured in one of these tests in order to determine all four creep compliances. This paper is more concerned with the development and initial results of an experiment designed to accomplish this task than with the complete characterization of the commercially available PET films.

The simultaneous measurement of the longitudinal extension and lateral contraction directly gives the Poisson's ratio:

$$\nu = -\frac{\Delta c_y/c_{0y}}{\Delta \ell_z/\ell_{0z}} \tag{5}$$

where  $\Delta c_y$  and  $\Delta \ell_z$  represent the changes in width and length of the PET test strip, respectively, and  $c_{0y}$  and  $\ell_{0z}$  are the original width and length, respectively, of the same strip. Since the change in width is much less than the change in length, the measurement of width change must be performed with much higher accuracy than the measurement of the length change. The longitudinal elongation is measured either by the method of optical microscopy [14] (with  $\ell_{0z}=200$  mm) or by using a Linear Variable Differential Transformer (LVDT) (with  $\ell_{0z}=900$  mm). Both methods are subsequently described in detail, and both provide a sufficiently high degree of resolution relative to the amounts of longitudinal elongation to

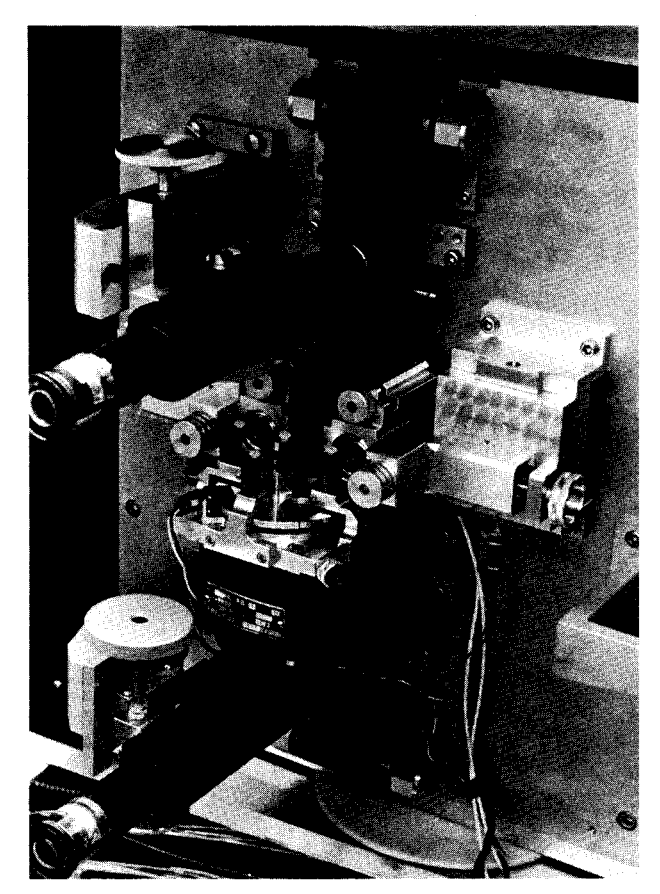


Figure 1 Front view of test apparatus with microscopes.

be measured. On the other hand, the measurement of the lateral contraction of specimens is achieved by means of a much higher resolution laser scanning technique, which is also subsequently described.

In order for the material response to remain in the linear range of the material, the longitudinal strain is kept below  $5 \times 10^{-3}$ . For an elastic modulus of  $4 \times 10^{9} \text{ N/m}^2$ and a specimen of 51-mm width and 25-\(\mu\)m thickness, this strain would be given by a load of 25.5 N. For a Poisson's ratio of 0.3, the same specimen would experience a total elastic width change (contraction) of  $7.6 \times 10^{-2}$  mm, or, equivalently, a movement of 38 µm at each edge. This figure would, of course, decrease with smaller loads and/ or thicker specimens. From our earlier experiments we have observed that the time-dependent component of the total creep in the first 30 hours under constant load is less than 40% of the instantaneous component. Assuming that the Poisson's ratio remains approximately constant during this period at around 0.3, we would get a movement of less than 16  $\mu$ m at each edge during a 30-hour time period. As we shall subsequently show, the optical-electronic system used to measure the lateral width change of test strips achieves an accuracy of  $\pm 0.8~\mu m$ , which meets the resolution requirements indicated by the calculations just described.

# Determination of longitudinal strain by optical microscopy

In this method of determination of longitudinal strain, the elongation of a 200-mm test section is measured. Two small horizontal scratches are scribed, 200 mm apart on the tape, perpendicular to the load direction. If the tape is coated, this is done in "windows" where the oxide coating has been removed. The scratches are longitudinally located several tape widths from any clamps or rollers to ensure uniaxial stress in the test section. The tape is mounted so that the scratches are near the tops of two microscope stage scales fixed to the apparatus behind the specimen. The scratches are located by use of two telescopes  $(200\times)$  mounted in front of the specimen (Fig. 1). As loading changes or as the specimen creeps, the movement of the scratches relative to the scales can be observed and recorded. Thus, the change in the length, and hence the axial strain of the originally 200-mm-long test section, is determined.

This measurement technique was originally employed because of its simplicity, reliability, and acceptability as a truly uniaxial tension test. In this investigation, it was used principally in experiments conducted for the purpose of determining the instantaneous Poisson's ratio under room temperature and humidity conditions. On the other hand, when a creep experiment is conducted in an environmental chamber, the technique becomes unwieldy as the chamber door has to be opened in order to take data. Therefore, an alternate longitudinal strain measuring scheme was devised and used in the experiments conducted for the determination of longitudinal creep in humidity- and temperature-controlled environments.

# Measurement of longitudinal strain with a Linear Variable Differential Transformer

In the LVDT method of determining the longitudinal strain, the elongation of a tape sample of about 900-mm length is measured from the position at which it is clamped to the position at which the load is applied. A schematic of the experimental set-up is illustrated in Fig. 2. The LVDT measures the travel of the loaded end of the specimen, which is used to obtain the longitudinal strain. Since the specimen is restrained from width contraction on both ends by the mounting clamps and also by four guidance rollers, some objections could be raised to the effect that the stress is not uniaxial. However, the rollers are very smooth and built with precision bearings and the tape length is 900 mm between end clamps. It is, therefore, reasonable to expect only small end effect errors in

measuring the longitudinal strain by the weight travel technique. Experiments were conducted in a normal laboratory environment for the purpose of comparing the longitudinal strains measured by the two techniques. The results were as indicated in Table 1 for a load of 4.5 N.

The discrepancy in each case is about 1%, implying, therefore, that the LVDT measurement is sufficiently accurate.

In addition to making possible remote operation inside an environmental chamber, the LVDT technique allows the obtaining of a continuous record of the longitudinal creep process. For these reasons, the LVDT technique was employed for the determination of the longitudinal strain in all of the creep experiments conducted.

#### Measurement of lateral strain

In this section, the laser-scanning technique used for the measurement of the lateral contraction of specimens is described. Figure 3 shows a schematic of the width measurement apparatus and Fig. 1 shows a front-view photograph. A 3-mW He-Ne laser is directed onto a rotating mirror by means of the two fixed mirrors M, and M, oriented at 45° to the beam direction. The angular speed of the rotating mirror is 1800 rpm, and for each revolution the fixed mirrors M<sub>3</sub> and M<sub>4</sub> are scanned by the laser beam. When these mirrors are scanned, their reflected beams sweep across the active area of the photodiodes PD1 and PD2. A test piece of PET and calibration slits of known width (0.356 mm on the left side and 0.350 mm on the right side) are arranged in front of each of the photodetectors so as to create two vertical gaps which can be swept horizontally by the laser beam. As the beam sweeps each gap, it produces a gate pulse whose width is proportional to the gap width. The gate pulse and the 20-MHz oscillator signal are combined, and the resulting output is sent to an electronic counter. The output from the counter is displayed by numerical readouts for each of the gaps. In the beginning of a test, a strip of PET is placed on the apparatus and slightly loaded to take out slack (L < 2.5 N). Then the counter readings are recorded for each of the four gaps. If  $C_1$  and  $C_2$  denote counter readings corresponding to the gap between the edge of the fixed frame and the edge of the strip on the left- and right-hand sides, and if  $C_2$  and  $C_3$  correspond to the calibration slit readings on the left- and right-hand sides, respectively, then the sum S of widths of the gaps between the fixed edges of the frame and the left and right edges of the strip is given by

$$S = \frac{0.356C_1}{C_2} + \frac{0.350C_4}{C_3}. (6)$$

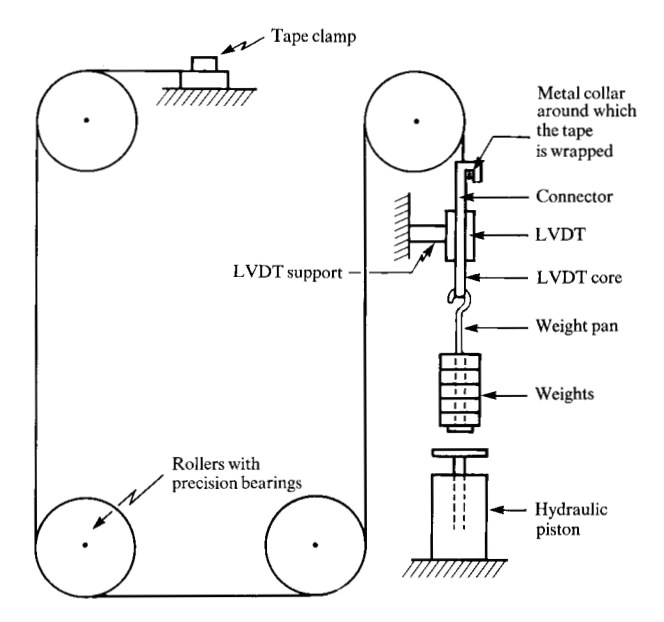


Figure 2 Schematic of experimental set-up for longitudinal strain measurement with LVDT.

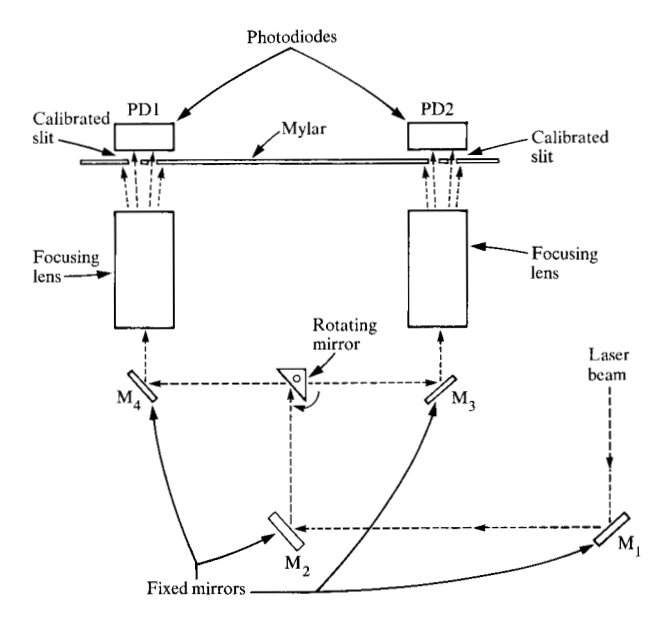


Figure 3 Schematic of scanning laser system.

Table 1 Comparison of longitudinal strain measured by different techniques.

Test	Strain (by telescope- scratch method) (mm/mm)	Strain (by LVDT method) (mm/mm)
#1	$4.59 \times 10^{-4}$	$4.66 \times 10^{-4}$
#2	$4.60 \times 10^{-4}$	$4.64 \times 10^{-4}$
#3	$4.54 \times 10^{-4}$	$4.60 \times 10^{-4}$

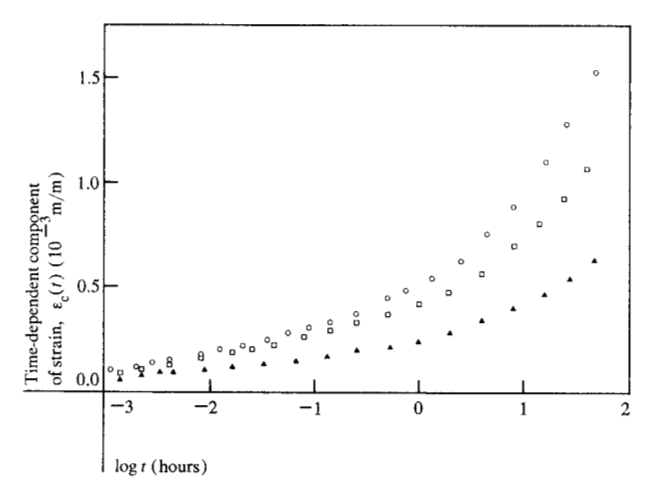


Figure 4 Dependence of creep of Mylar on load (linearity test). 25-μm CrO₂-coated tapes;  $T = 45^{\circ}$ C; relative humidity = 50%. ○ Load = 23.64 N (1.86 × 10<sup>7</sup> N/m²) −100% −ε₀ = 0.003664. □ Load = 18.84 N (1.48 × 10<sup>7</sup> N/m²) −80% −ε₀ = 0.003088. ▲ Load = 10.55 N (0.83 × 10<sup>7</sup> N/m²) −45% −ε₀ = 0.001595.

Table 2 Sample readings for lateral strain measurement.

t	$C_{_1}$	$C_4$	$C_2$	$C_3$
0	378	370	402	386
$t_0$	384	375	402	385

Table 3 Instantaneous Poisson's ratio.

Test	Poisson's ratio
#1	0.242
#2	0.229
#3	0.232
#4	0.221

The following numerical example illustrates the determination of lateral strain. Assume that the readings are taken from  $C_1$ ,  $C_2$ ,  $C_3$ , and  $C_4$  at t=0 and again at  $t=t_0$  (after either the loading has been changed or a measurable amount of creep has taken place), and that the results are as given in Table 2. Then the sums of the two gaps between the fixed frame and the contracting PET edges are given by

S(0) = 0.6704 mm

and

$$S(t_o) = 0.6810 \text{ mm}.$$
 (7)

Thus,  $S(t_0) - S(0)$ , the amount by which the width of the specimen has contracted between t = 0 and  $t = t_0$ , equals 0.0106 mm. The negative of this amount divided by the original width of the strip (50 mm) gives the additional lateral strain experienced by the specimen in the time interval from t = 0 to  $t = t_0$ .

#### • Determination of instantaneous Poisson's ratio

The first experiments were performed to measure the instantaneous Poisson's ratio of PET under room conditions. In these experiments, the uniaxial loading on the PET strips was increased in increments of about 5 N and the longitudinal and lateral strain changes from an initial slightly loaded (2.5 N) reference configuration were measured for each loading. The longitudinal strain was measured by the method of optical microscopy, and the laser-scanning technique was used for the measurement of lateral strain. These two strain measurements were each plotted against the applied stress. The ratio of the slope of the lateral strain vs. stress to the slope of the longitudinal strain vs. stress gives the Poisson's ratio.

Reproducibility of the results was checked by repeating the test just described several times on the same 38.1- $\mu$ m-thick tape. The data obtained are illustrated in Table 3. These results fall within the anticipated accuracy range of  $\pm 5\%$ .

The creep of the PET during each test is negligible as compared to the magnitude of strain changes caused by the loading increments. Therefore, the heretofore described results can safely be considered to be free of viscoelastic influences.

### Linearity of material response

The time-dependent longitudinal strain experienced by the strip under constant load is expressed as the sum of the instantaneous and the time-dependent components,

$$\varepsilon(t) = \varepsilon_0 + \varepsilon_c(t), \quad [\varepsilon_c(0) = 0].$$

Since we propose to use linear theory (1), the question to be resolved is whether or not  $\varepsilon(t)$  depends linearly on the applied load. Since the instantaneous Poisson's ratio measurements have shown that the  $\varepsilon_0$  component is linear, it remains to check the linearity with respect to load of the  $\varepsilon_c(t)$  component.

In these creep-linearity tests,  $\text{CrO}_2$ -coated Mylar [15] strips of 25- $\mu$ m thickness were used. The temperature and relative humidity were maintained at 45°C and 50%, respectively, and the longitudinal strain measurements were carried out using the LVDT technique. The applied loads for the three creep tests were 23.64 N, 18.84 N and

10.55 N (corresponding to stresses of  $1.861 \times 10^7$ ,  $1.483 \times 10^7$ , and  $0.831 \times 10^7 \text{ N/m}^2$ ) for three specimens cut in the machine direction at the same location across the roll. The values of  $\varepsilon_0$  measured for the three loads were 0.003664, 0.003088, and 0.001595, respectively. The results for  $\varepsilon_c(t)$  are shown in Fig. 4 plotted on a logarithmic time scale. These plots show that  $\varepsilon_{c}(t)$  is approximately a linear function of the loads for this sample in this load range. The smaller loads are 80% and 45% of the larger load, and the  $\varepsilon_c(t)$  for them varies within ranges 74-85% and 41-49%, respectively, of the  $\varepsilon_{c}(t)$  for the larger load in the first 32 hours of measurement. The corresponding ratios for the  $\varepsilon_0$  values are 84% and 44%.

• Time-temperature dependence of longitudinal creep The objective of the experiments which will next be described was to demonstrate the time-temperature superposition hypothesis on the longitudinal creep of Mylar (see also [4]), and an additional objective was to check our measurements against earlier data obtained by T. Smith [7] using a different method.

According to the time-temperature superposition hypothesis, the time-dependent longitudinal creep data  $\varepsilon(t)$ , for tests conducted at different temperatures with the same loading, type of specimen, and relative humidity, will coincide if the data are shifted along the logarithmic time axis by appropriate amounts  $\log a_x$ . Here, the creep is plotted in the more convenient form  $6 + \log D(t) vs$ . log t, where  $D(t) = \varepsilon(t)/\sigma$  is the creep compliance and  $\sigma$ is the constant uniaxial stress. To effect complete superposition, it is usually necessary to shift the curves by small amounts  $\log c_r$  along the  $[6 + \log D(t)]$ -axis, thus accounting for the run-to-run variability in the D(t) data at different temperatures. The values for  $\log a_r$  were found experimentally by Smith [7] to conform to the equation

$$\log a_T = -0.102(T - 309),\tag{8}$$

where the temperature T is expressed in K and the reference temperature is 36°C.

Four tests were conducted at the temperatures 36°C, 45°C, 55°C, and 65°C, respectively, all at 50% relative humidity. The specimens used were clear (uncoated) 35.5μm-thick Mylar 142 PB, and the applied tensile stress was  $7.86 \times 10^6 \text{ N/m}^2$  in each test. These specimens were taken from the same stock on the same side of the web as those used by Smith in his test [7]. The applied stress was also the same. However, there was a significant difference in the specimen sizes between the two sets of creep tests. As mentioned earlier, the Berkeley tests used 50  $\times$ 900-mm specimens while the San Jose tests used 3.3  $\times$ 7.4-mm specimens in a du Pont TMA tester. The temperatures of the Berkeley and San Jose tests were the same

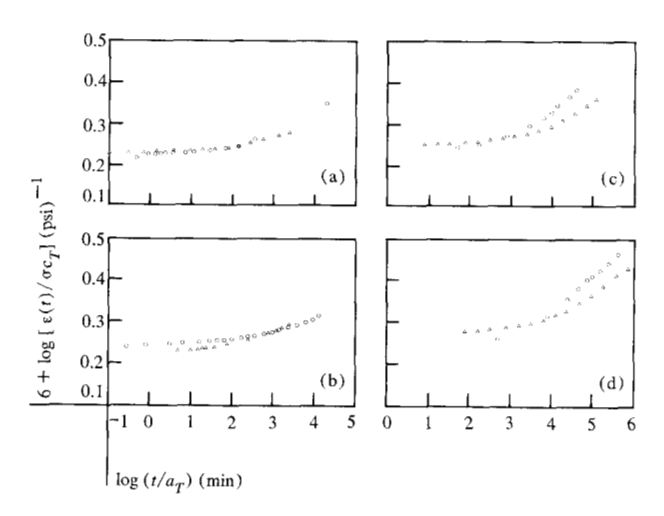


Figure 5 Longitudinal creep of Mylar at constant temperature. 35.5-µm Mylar 142 PB (uncoated); relative humidity = 50%; tensile stress =  $7.86 \times 10^6 \text{ N/m}^2$ .  $\bigcirc$ , San Jose data;  $\triangle$ , Berkeley

- (a)  $T = 36^{\circ}$ C.  $\log a_T = 0$ ,  $c_T = 1$  (Berkeley).

- (b)  $T = 45^{\circ}\text{C.} \log a_T = -0.918, c_T = 1 \text{ (Berkeley)}.$ (c)  $T = 55^{\circ}\text{C.} \log a_T = -1.938, c_T = 1 \text{ (Berkeley)}.$ (d)  $T = 65^{\circ}\text{C.} \log a_T = -2.958, c_T = 1 \text{ (Berkeley)}.$

but the relative humidity was not controlled in the San Jose tests. The results of the longitudinal creep are shown in Figs. 5(a)-(d). Also plotted there are the corresponding longitudinal creep data in the optical transverse direction (TOX) as supplied by Smith [7]. In transferring these data to Fig. 5, the shift factor  $a_r$  had to be applied. Some error in transmitting the data is possible due to the fact that the correction factors log  $c_r$  for the 36°C, 55°C, and 65°C runs were not available. We know, however, that  $0 < \log c_r <$ 0.089. The results show that the Berkeley and San Jose data are in close agreement. The largest discrepancy is about 17% at 55°C after 8.75 hours. This could possibly be accounted for by humidity differences.

All the Berkeley data are plotted in a master curve in Fig. 6, which shows that, within small adjustments  $(-0.008 < \log c_T < 0.015)$ , the time-temperature superposition hypothesis appears to apply even though the temperatures are below the glass transition temperature of 65°C.

### Creep data

The elongation and lateral contraction of Mylar strips under constant loads in temperature- and humidity-controlled environments were measured simultaneously using the LVDT and laser-scanning methods in tests of duration of more than 30 hours. Eight tests were carried out to complete a matrix covering two kinds of specimens, two temperatures and two constant loads. The types of

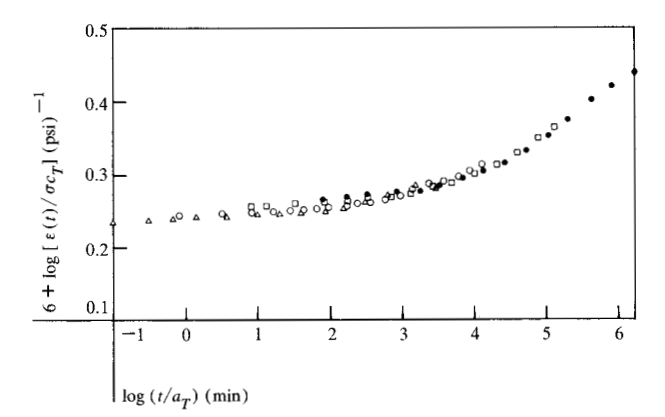


Figure 6 Time-temperature superposition of Berkeley data from Figs. 5(a)-(d).

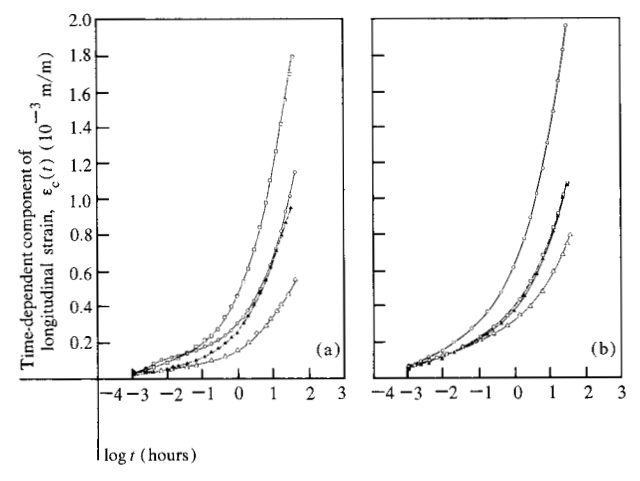


Figure 7 Time-dependent component of longitudinal strain. Relative humidity = 50%;  $\varepsilon_0$  = "instantaneous" strain component. (a) uncoated tape:

 $\Box T = 55^{\circ}\text{C. Load} = 28.45 \text{ N} (1.58 \times 10^{7} \text{ N/m}^2). \ \varepsilon_0 = 4.628 \times 10^{7} \text{ N/m}^2$ 

 $\Delta T = 45^{\circ}$ C. Load = 28.45 N (1.58 × 10<sup>7</sup> N/m<sup>2</sup>).  $\varepsilon_0 = 3.37$  ×

 $\bigcirc T = 55^{\circ}\text{C. Load} = 18.84 \text{ N } (1.04 \times 10^{7} \text{ N/m}^{2}). \ \varepsilon_{0} = 2.265 \times 10^{10} \text{ N/m}^{2}$  $10^{-3}$ 

 $\triangle T = 45^{\circ}\text{C. Load} = 18.84 \text{ N} (1.04 \times 10^{7} \text{ N/m}^{2}). \ \varepsilon_{0} = 2.04 \times 10^{-3}.$ (b) coated tape:

 $O T = 55^{\circ}C$ . Load = 23.64 N (1.86 × 10<sup>7</sup> N/m<sup>2</sup>).  $\varepsilon_0 = 3.659$  ×

 $\Box T = 55^{\circ}\text{C. Load} = 16.35 \text{ N} (1.29 \times 10^{7} \text{ N/m}^{2}). \ \varepsilon_{0} = 2.339 \times 10^{7} \text{ N/m}^{2}$ 

 $\Delta$  T = 45°C. Load = 23.64 N (1.86 × 10<sup>7</sup> N/m²).  $\varepsilon_0$  = 3.44 × 10<sup>-3</sup>.  $\Delta$  T = 45°C. Load = 16.35 N (1.29 × 10<sup>7</sup> N/m²).  $\varepsilon_0$  = 2.303 × 10<sup>-3</sup>

Mylar films used were CrO<sub>2</sub>-coated films of 25-μm thickness and uncoated films of 35.5-µm thickness. The two temperatures chosen were 45°C and 55°C. For CrO<sub>3</sub>coated specimens, tests were run at constant loads of  $1.862 \times 10^7 \text{ N/m}^2$  and  $1.288 \times 10^7 \text{ N/m}^2$  at each temperature, whereas the uncoated specimens were tested under loads of  $1.044 \times 10^7 \text{ N/m}^2$  and  $1.576 \times 10^7 \text{ N/m}^2$  at each temperature.

During the course of trial experiments, it was observed that the lateral creep data were extremely sensitive to imperfections in the initial configuration of the Mylar sample. In order to achieve a high degree of reproducibility, great care was taken to ensure that the mounting of the specimen was performed correctly. In addition, tests checking the linearity of lateral contraction as a function of loading were conducted before and after each creep process. These tests were similar to those carried out for the purpose of determining the instantaneous Poisson's ratio. They were conducted under room conditions and with small loads only, so that the stress history put into the specimen would be minimal. The post-creep linearity tests, on the other hand, were carried out for larger loads and at the same temperatures and humidity conditions as the creep test. Only creep data from specimens that showed linearity of lateral contraction with respect to load prior to and after the conclusion of the creep test were deemed acceptable.

To ensure that the creep was being measured under steady-state conditions, each specimen was maintained in the environmental chamber at the designated temperature and relative humidity for about 13 hours before the constant load was applied.

Figures 7(a) and (b) are plots of the time-dependent component of the longitudinal strain,  $\varepsilon_c(t)$ , as a function of time for a coated and an uncoated tape sample, respectively. The value of the instantaneous component  $\varepsilon_0$  for each test is also recorded.

Figures 8(a) and (b) are plots of the negative of the time-dependent component of lateral strain for the coated and uncoated tape samples, respectively. The vertical bars reflect the digital nature of the read-out and may be interpreted as regions of uncertainty. Again, the value of the instantaneous component  $\varepsilon_0$  is indicated for each case.

Finally, Figs. 9(a) and (b) are plots of the Poisson's ratio,  $\nu(t)$ , as a function of time for the coated and uncoated samples, respectively. The values of the static Poisson's ratio  $\nu_0$  and the range of percentage of  $\nu_0$ , within which  $\nu(t)$  falls for the duration of the tests, are given as a measure of the validity of a possible constant function approximation  $\nu(t) = \nu_0$ . For both the coated and uncoated tapes, it is a good approximation to use the instantaneous value of the Poisson's ratio for the time-dependent creep value.

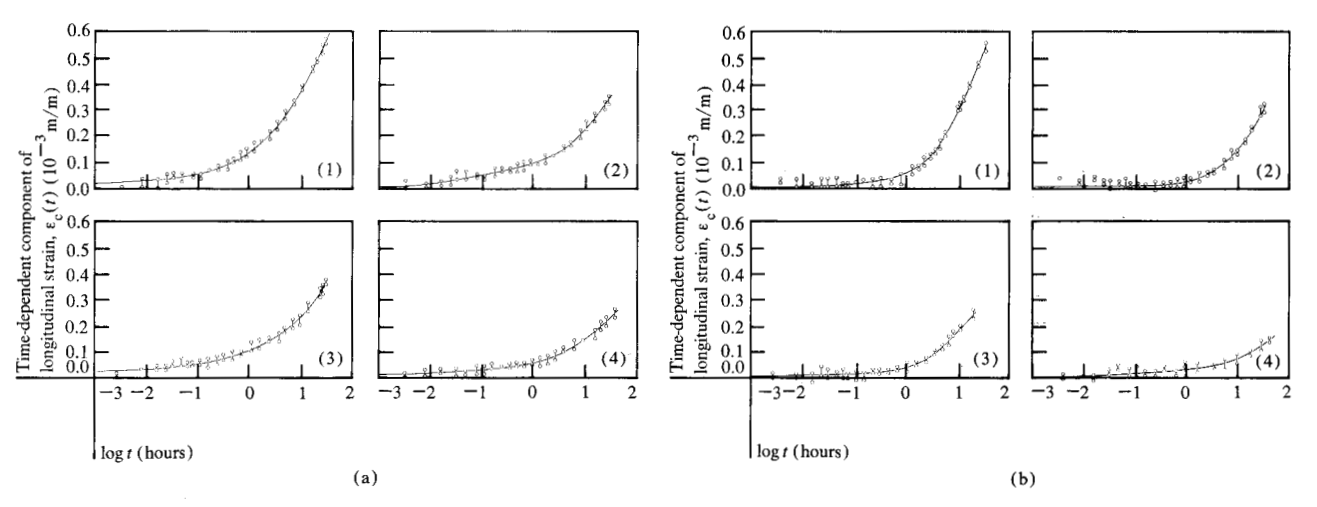


Figure 8 (a) Time-dependent lateral strain (coated tape). Relative humidity = 50%; 25-μm CrO<sub>2</sub>-coated tape.

- (1)  $T = 55^{\circ}\text{C}$ . Load = 23.64 N (1.86 × 10<sup>7</sup> N/m<sup>2</sup>),  $\varepsilon_0 = -0.975 \times 10^{-3}$ . (2)  $T = 55^{\circ}\text{C}$ . Load = 16.35 N (1.29 × 10<sup>7</sup> N/m<sup>2</sup>).  $\varepsilon_0 = -0.674 \times 10^{-3}$ .
- (3)  $T = 45^{\circ}\text{C}$ . Load = 23.64 N (1.86 × 10<sup>7</sup> N/m<sup>2</sup>).  $\varepsilon_0 = -0.95 \times 10^{-3}$ . (4)  $T = 45^{\circ}\text{C}$ . Load = 16.35 N (1.29 × 10<sup>7</sup> N/m<sup>2</sup>).  $\varepsilon_0 = -0.655 \times 10^{-3}$ .
- (b) Time-dependent lateral strain (uncoated tape). Relative humidity = 50%; 35.5- $\mu$ m uncoated tape. (1)  $T = 55^{\circ}$ C. Load = 28.45 N (1.58 × 10<sup>7</sup> N/m<sup>2</sup>).  $\varepsilon_0 = -0.736 \times 10^{-3}$ . (2)  $T = 55^{\circ}$ C. Load = 18.84 N (1.04 × 10<sup>7</sup> N/m<sup>2</sup>).  $\varepsilon_0 = -0.488 \times 10^{-3}$ .

- (3)  $T = 45^{\circ}\text{C}$ . Load = 28.45 N (1.58 × 10<sup>7</sup> N/m<sup>2</sup>).  $\varepsilon_0^0 = -0.77 \times 10^{-3}$ .
- (4)  $T = 45^{\circ}\text{C}$ . Load = 18.81 N (1.04 × 10<sup>7</sup> N/m<sup>2</sup>).  $\varepsilon_0^{\circ} = -0.511 \times 10^{-3}$ .

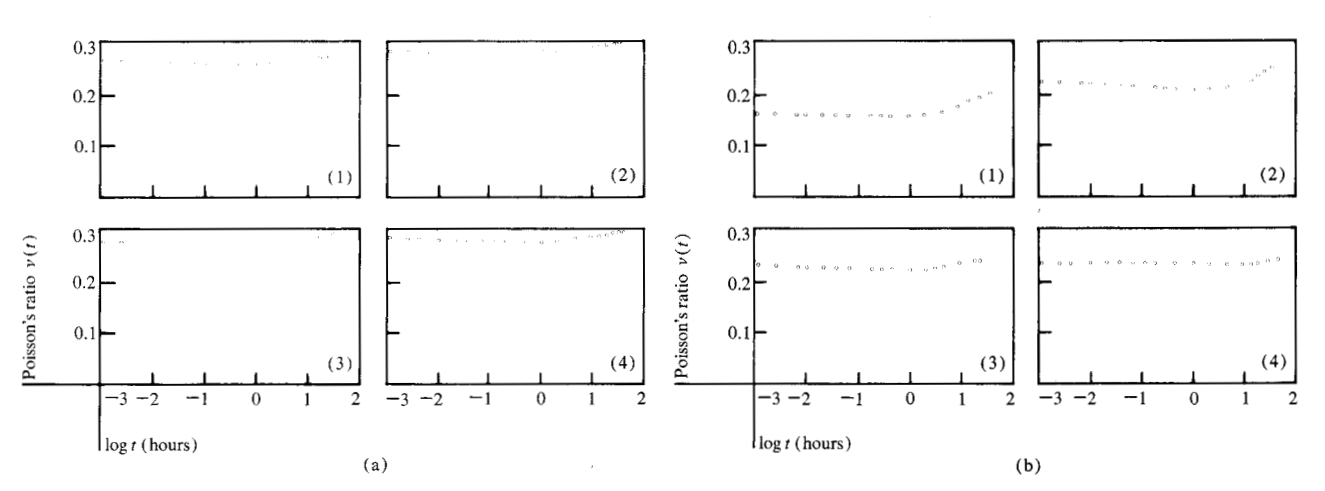


Figure 9 (a) Poisson's ratio as a function of time (coated tape). 25-μm CrO<sub>α</sub>-coated tape; relative humidity = 50%.

- (1)  $T = 55^{\circ}$ C. Load = 23.64 N (1.86 × 10<sup>7</sup> N/m<sup>2</sup>).  $\nu_0 = 0.266$ . Range of percentage of  $\nu_0$ : 97-103%. (2)  $T = 55^{\circ}$ C. Load = 16.35 N (1.29 × 10<sup>7</sup> N/m<sup>2</sup>).  $\nu_0 = 0.2881$ . Range of percentage of  $\nu_0$ : 98-104%. (3)  $T = 45^{\circ}$ C. Load = 23.64 N (1.86 × 10<sup>7</sup> N/m<sup>2</sup>).  $\nu_0 = 0.276$ . Range of percentage of  $\nu_0$ : 99-106%. (4)  $T = 45^{\circ}$ C. Load = 16.35 N (1.29 × 10<sup>7</sup> N/m<sup>2</sup>).  $\nu_0 = 0.285$ . Range of percentage of  $\nu_0$ : 96-102%.

- (b) Poisson's ratio as a function of time (uncoated tape). 35.5-μm uncoated tape; relative humidity = 50%.
- (1)  $T = 55^{\circ}$ C. Load = 28.45 N (1.58 × 10<sup>7</sup> N/m<sup>2</sup>).  $\nu_0 = 0.159$ . Range of percentage of  $\nu_0$ : 98-126%. (2)  $T = 55^{\circ}$ C. Load = 18.84 N (1.04 × 10<sup>7</sup> N/m<sup>2</sup>).  $\nu_0 = 0.2155$ . Range of percentage of  $\nu_0$ : 94-115%. (3)  $T = 45^{\circ}$ C. Load = 28.45 N (1.58 × 10<sup>7</sup> N/m<sup>2</sup>).  $\nu_0 = 0.2285$ . Range of percentage of  $\nu_0$ : 96-109%. (4)  $T = 45^{\circ}$ C. Load = 18.84 N (1.04 × 10<sup>7</sup> N/m<sup>2</sup>).  $\nu_0 = 0.251$ . Range of percentage of  $\nu_0$ : 97-107%.

## Discussion and conclusions

The time-dependent creep functions for "as-received" Mylar were obtained under carefully controlled conditions so that an experimental error of less than 10% should be expected. However, since stress relaxation of the material starts immediately after the drawing process, it is apparent that "as received" Mylar samples will always be in a different state of stress relaxation depending

on the time elapsed since manufacturing. Thus, depending on the age of the Mylar, we may expect different samples to give different results in the creep tests. Although in the present study this latter complication was avoided by taking the samples from the same tape, we point out that a larger experimental spread is to be expected for tape samples whose prior history is unknown.

In deriving the creep functions from our experiments, we have made use of the time-temperature superposition hypothesis and found that the test results at varying temperatures can be nicely arranged in a master curve. The time-temperature superposition hypothesis is usually assumed to be valid only for temperatures above the glass transition temperature [2]. However, the data of Smith [7] as well as the data of this study indicate that good results are obtained using this hypothesis at temperatures below the glass transition temperature. We have no evidence that this is universally valid, and further research should be directed toward this particular finding.

From the experiments described here, we can conclude that the Poisson's ratio is, to a first approximation, time independent. This result is of significance since it greatly simplifies analytical calculations and also reduces the experimental effort needed in characterizing anisotropic thin sheets. However, the generalization of this result should be considered carefully in view of our limited sample size, and further research, especially with other materials, appears to be warranted and highly desirable.

#### References and notes

- 1. "Physical and Thermal Properties of du Pont Mylar Polyester Film," *Technical Information Bulletin M-2D*, E. I. du Pont de Nemours and Co., Inc., Wilmington, DE.
- I. M. Ward, Mechanical Properties of Solid Polymers, Wiley-Interscience, New York, 1971.

- 3. M. W. Darlington and D. W. Saunders, "The Tensile Creep Properties of Cold-Drawn Low-Density Polyethelene," J. Phys. D.: Appl. Phys. 3, 535-549 (1970).
- M. W. Darlington and D. W. Saunders, "The Anisotropy of Creep Behavior in Oriented Thermoplastics," *Polymer Eng.* Sci. 14, 616-620 (1974).
- T. Marayama, J. H. Bumbleton, and M. L. Williams, "Viscoelasticity of Oriented Poly(ethylene Terephthalate)," J. Polymer Sci. (Part A-2) 6, 787-793 (1968).
- E. M. Barrall II and J. A. Logan, "Some Properties of Biaxially Oriented Poly(ethylene Terephthalate)," Research Report RJ 1223, IBM Research Division laboratory, San Jose, CA, 1973.
- T. L. Smith, June 1974, IBM Research Division, San Jose, CA, private communication.
- E. A. Bartkus, July 1974, IBM General Products Division, Tucson, AZ, private communication.
- E. A. Bartkus and R. L. Price, IBM Technical Report TR 44.0244, June 15, 1973.
- D. B. Bogy, unpublished results, IBM Research Division laboratory, San Jose, CA, 1974.
- H. J. Greenberg, "Dimensional Stability of Flexible Disks, Experimental Results," Research Report RJ 1676, IBM Research Division laboratory, San Jose, CA, 1975.
- S. G. Lekhnitskii, Theory of Elasticity of an Anisotropic Elastic Body, Holden-Day Series in Mathematical Physics, Holden-Day, Inc., San Francisco, 1963.
- R. M. Christensen, Theory of Viscoelasticity, Academic Press, Inc., New York, 1971.
- R. Stephens, "Long Term Effects of Temperature and Humidity on Flexible Substrates," September 1975, IBM Research Division, San Jose, CA, private communication.
- "Mylar" is a registered trademark of E. I. du Pont de Nemours and Co., Inc., Wilmington, DE.

Received October 27, 1978; revised December 22, 1978

D. B. Bogy and N. Bugdayci are located at the University of California, Berkeley, California 94720; F. E. Talke is located at the IBM Research Division laboratory, 5600 Cottle Road, San Jose, California 95193.